AD-A168 498 HOLOGRAPHIC OPTICAL ELEMENTS FORMED IN LIGHT OF REDUCED COHERENCE(U) MICHIGAN UNIV ANN ARBOR DEPT OF ELECTRICAL AND COMPUTER ENGIN E LEITH 27 FEB 86 1/1

UNCLASSIFIED AFOSR-TR-86-0324 AFOSR-85-0012 F/G 14/5 NL

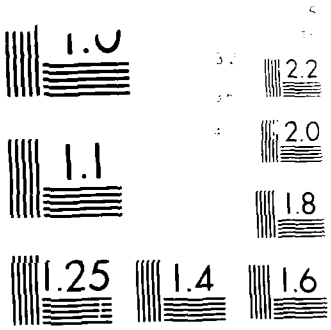
1.0
2.2
2.0
1.1
1.8
1.25
1.4
1.6

Report No. 7

Annual Report for Period Nov. 30, 1984 to Nov. 30, 1985

Holographic Optical Elements Formed in Light of Reduced Coherence

Sponsored by
Air Force Office of Scientific Research
Grant No. AFOSR 850012

The University of Michigan
Department of Electrical and Computer Engineering
Ann Arbor, Mich.

Feb. 1986

Unclassified
SECURITY CLASSIFICATION OF THIS PAGE

REPORT DOCUMENTATION PAGE

1a. REPORT SECURITY CLASSIFICATION
unclassified

1b. RESTRICTIVE MARKINGS

2a. SECURITY CLASSIFICATION AUTHORITY

2b. DECLASSIFICATION / DOWNGRADING SCHEDULE

3. DISTRIBUTION / AVAILABILITY OF REPORT

4. PERFORMING ORGANIZATION REPORT NUMBER(S)
Report No. 7

5. MONITORING ORGANIZATION REPORT NUMBER(S)
[illegible]

6a. NAME OF PERFORMING ORGANIZATION
Univ. of Mich

6b. OFFICE SYMBOL *(If applicable)*

7a. NAME OF MONITORING ORGANIZATION
[illegible]

6c. ADDRESS *(City, State, and ZIP Code)*
Ann Arbor, Mich, 48109

7b. ADDRESS *(City, State, and ZIP Code)*

8a. NAME OF FUNDING / SPONSORING ORGANIZATION
AFOSR

8b. OFFICE SYMBOL *(If applicable)*
NP

9. PROCUREMENT INSTRUMENT IDENTIFICATION NUMBER
[illegible]

8c. ADDRESS *(City, State, and ZIP Code)*
Bolling Air Force Base, D.C. 20332

10. SOURCE OF FUNDING NUMBERS

PROGRAM ELEMENT NO	PROJECT NO	TASK NO.	WORK UNIT ACCESSION NO
	2305	B1	

11. TITLE *(Include Security Classification)*
Holographic Optical Elements Formed in Light of Reduced Coherence

12. PERSONAL AUTHOR(S)
E. Leith

13a. TYPE OF REPORT
annual

13b. TIME COVERED
FROM [illegible] TO [illegible]

14. DATE OF REPORT *(Year, Month, Day)*
1986, Feb. 27

15. PAGE COUNT
37

16. SUPPLEMENTARY NOTATION

17. COSATI CODES

FIELD	GROUP	SUB-GROUP
20	06	

18. SUBJECT TERMS *(Continue on reverse if necessary and identify by block number)*
hologram, optical element, interferometry, spatial filtering

19. ABSTRACT *(Continue on reverse if necessary and identify by block number)*

The theory of holographic optical elements made with light of reduced coherence is developed. Both reduced spatial coherence and temporal coherence methods are considered. A theory of broad source fringe formation based on source-image distortion is developed. The theory of HOE formation with two zone plates in tandem and under reduced temporal coherence is developed. A new technique of spatial filtering with spatially incoherent light was developed in which the optical system behaves as if the light were coherent (i.e., linear in amplitude and phase preserved) even though the light is spatially incoherent. A technique for obtaining resolution beyond the classical limit (superresolution) was discovered, based on the principle of incoherent to coherent conversion.

20. DISTRIBUTION / AVAILABILITY OF ABSTRACT
☒ UNCLASSIFIED/UNLIMITED ☐ SAME AS RPT ☐ DTIC USERS

21. ABSTRACT SECURITY CLASSIFICATION
unclassified

22a. NAME OF RESPONSIBLE INDIVIDUAL
Lt. Col. Robert Carter,Jr

22b. TELEPHONE *(Include Area Code)*
(202) 767-4931

22c. OFFICE SYMBOL

DD FORM 1473, 84 MAR

83 APR edition may be used until exhausted
All other editions are obsolete

SECURITY CLASSIFICATION OF THIS PAGE
Unclassified

1. Research Objectives

Our research objectives, as stated in the work statement of our proposal, were:

1. develop methods for providing low noise optical elements by interferometric means, including gratings, lenses, beam combiners, corrector plates, and other special elements, such as circular, eliptical and hyperbolic axicon lenses, including the following tasks:

   (a) apply the Lau effect in combination with spatial filtering to produce nonsinusoidal fringe distributions

   (b) compare the broad spectrum with the broad source techniques for HOE generation

   (c) seek methods for making HOEs in light that is simultaneously spatially and spectrally incoherent

   (d) using higher order analysis, study the aberrations of incoherent light HOEs, and methods to reduce aberration

   (e) determine methods for producing fringes under conditions of greatest possible incoherence, including determining any required departure from sphericity of the interfering waves

   (f) develop methods for producing HOEs having arbitrary fringe spacings, instead of only linear and quadratic, thereby producing aspheric HOEs, as well as arbitrary phase plates

   (g) determine the usefulness of sources with structured spatial or spectral distributions in HOE construction

   (h) assess the limitation on space bandwidth product of incoherent light HOEs

   (i) develop a comprehensive theory for the construction of HOE lenses in light of reduced temporal coherence

2. Continue our basic investigations, with the intent of discovering new principles and techniques in the area of optical processing with light of reduce coherence.

2. Accomplishments

We have, during the past year, given attention to all of the above, with some of the objectives being investigated more intensively than others. Our principal accomplishments have been:

1. We continued our work on the basic treatment of HOE generation with spatially incoherent light and developed a theory of broad source interferometry based on source distortion. We showed that for an interferometer to give broad source fringes, the interferometer must form distorted images of the source. The grating interferometer introduces exactly the correct distortion, the Mach Zehnder gives no distortion at all, hence has very limited broad source capability.

A-1

2. We extended the theory of achromatic interferofmetry for HOE formation. We generalized the theory of the two zone plate interferometer for HOE formation.
3. We developed a merit factor for describing how well an incoherent source can produce a HOE
4. We developed a new method of spatial filtering using extended source incoherent light. The new system acts on the amplitude transmittance of the object transparency, and is therefore essentially a coherent system, even though the light is incoherent.
5. We developed a new technique for exceeding the classical resolution limit in an imaging system (a process sometimes called superresolution). We showed that if we have a two-branch interferometer producing broad source fringes, and if we have an imaging system in each branch, and then, if we place an object transparency in one branch and reduce the aperture of this imaging system to a very small value while retaining a large aperture for the empty branch, then the resolution achieved is that corresponding to the larger aperture, even though light from the object passes through only the small aperture, not the large one.

3

Generalization of the Two-Zoneplate Method of Achromatized HOE Formation

Introduction

The construction of Holographic Optical Elements (HOEs) has recently become an important area of research. Applications of HOEs such as heads up displays, supermarket scanners, and diode laser collimators have become increasingly widespread. The study of aberrations and noise of HOEs are two important topics of research. In this paper we discuss techniques for analysis and construction of low noise, zone plate HOEs. Low noise HOEs have been created by reducing the spatial coherence of the illuminating laser source[1,2] or by using a source of reduced temporal coherence[3]. This paper discusses the theory for analysis and construction of HOEs made by the latter technique, that is, HOEs made with a polychromatic point source.

Optical systems have been designed to make holograms in polychromatic point source illumination[4,5]. The optical systems discussed by Katyl[4] result in either on-axis or off-axis holograms. The on-axis technique is limiting. We would like to generate holograms of arbitrary center spatial frequency. The off-axis techniqueof Katyl images a grating to the recording plane, resulting in a hologram that is noise limited by this grating. One would like to be able to produce off axis HOEs of arbitrary center spatial frequency, but not at the expense of imaging noise planes, such as a grating, to the recording plane. Or, stated somewhat differently, the plane of fringe formation should not be an image plane for some physical structure, such as a grating, located upstream.

The optical setup described by Collins[5], employing a grating interferometer, was shown to be ideal for generating HOEs of this nature[3]. However, these zone plate HOEs were limited to interference between a plane wave and a spherical wave. Ideally, one would like to interfere waves of arbitrary curvature. This is a result of the aberrations inherent in a hologram when it is not used in exactly the same manner in which it was constructed[6]. Specifically, we would like to interfere a diverging wave with a converging wave. This is the only case that cannot be done cleanly with coherent light, since it necessitates at least one lens being introduced into one of the beams downstream from a pinhole, causing noise in the form of diffraction patterns of dust or other scatterers on the lens. With the use of polychromatic illumination these diffraction patterns can be smeared into a negligible background.

It is possible to construct zone plate lenses, as described above, with an arbitrary set of conjugate focal planes and arbitrary center spatial frequency, by generalizing the Katyl-Collins achromatic holographic system[3]. We shall see that by either moving or removing the final lens of Collins' system (Fig. 1) we will be able to construct zone plate lenses, although of limited space bandwidth product, in polychromatic light.

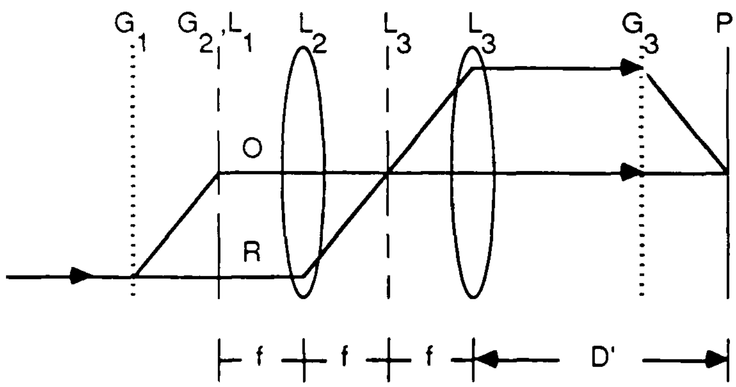

Fig. 1. The system described by Collins, consisting of the grating interferometer and a four/two lens system illuminated by a plane wave.

Requirements for Achromaticity

The analysis for the construction of zone plate lenses in polychromatic point source illumination is formulated in terms of the zone theory of Fresnel in conjunction with the Newtonian lens equation. The radius of the m^{th} zone of a Fresnel zone plate is given

$$R_m{}^2 = m\lambda F \qquad m = 1,2,3 \ldots \qquad (1).$$

We see that the radius of the m^{th} zone is directly proportional to the wavelength. As a consequence, the zone plate so constructed will exhibit a focal length F inversely proportional to wavelength, as in Fig. 2, resulting in wavelength dispersed point images. Reciprocity occurs when we construct a zone plate interferometrically, by

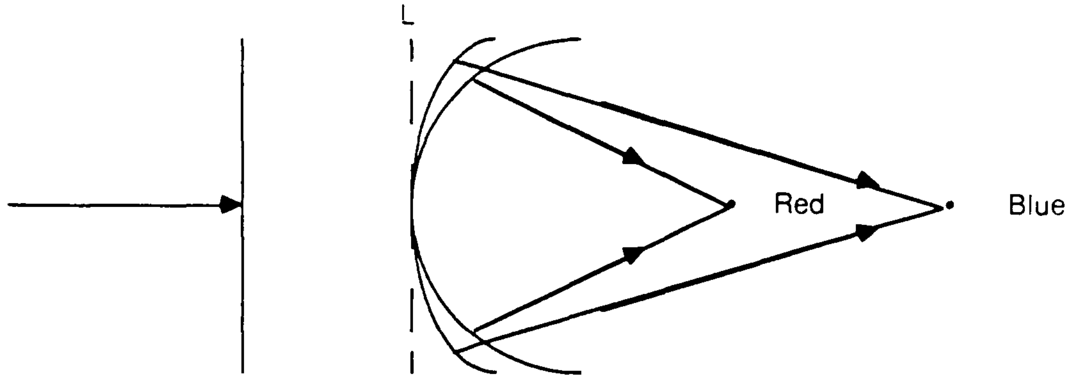

Fig. 2 A polychromatic plane wave hits an interferometrically recorded zone plate and is dispersed accordding to the formula $F=F_0(\lambda_0/\lambda)$. Where F_0 is the focal length at the midband wavelength λ_0.

interfering a plane and a spherical wave. If the spherical wave originates from a single point a distance F from the recording plane, the zones of constructive interference will have radii proportional to wavelength. However, if the point source is dispersed in such a way that the point source to recording plane distance is inversely proportional to wavelength, then each wavelength will make exactly the same zone plate. We seek a method by which we can make this wavelength dependence approximately constant over some wavelength band. From Eq. 1 we see that the only possibility for providing wavelength compensation is through F, the effective focal length of the zone plate being constructed. By manipulating the parameters that determine F, namely the radii of curvature of the two interfering beams, we can cause it to vary inversely with wavelength in an approximate fashion. We know F is given in terms of the relation,

$$1/F = 1/r_1 + 1/r_2 \qquad (2),$$

where r_1 and r_2 are the radii of curvature of the two interfering spherical waves and may be functions of wavelength. We can generate arbitrary radii of curvature with the desired wavelength variation by use of zone plate lenses in an optical system

We obtain the radius of curvature of a wave by finding the location of the plane at which the source is imaged. This location is in general a function of wavelength, determined by the focal lengths of the zone plates involved in the optical system. Once this plane is located we back up or go forward from it to the appropriate location for the particular HOE design. The distance of this move is one of the radii of curvature described above, and is also, in general, a function of wavelength. This technique of analysis is best illustrated by example and will be in the following sections.

One might notice that throughout this discussion no mention of actual physical pathlengths has ever been made. This comes about for two reasons. First, the grating interferometer, which splits and recombines the light, is inherently, minus all lenses, an achromatic system[7]. Second, both beams pass through the same optical elements in the system and because of this travel the same optical paths. The difference in sphericity of the two beams is generated by the use of zone plate lenses which allow a particular beam to be affected by the spherical phase transformation that is present on the plate, while the other beam is unaffected. This type of system, when analyzed using the above constraints, is used to produce zone plate lenses in polychromatic illumination.

A Four Lens System

Our analysis for the construction of HOEs with polychromatic illumination starts with the achromatic Fourier transforming system of Collins (Fig. 1). It was shown in Ref. 3 that off axis zone plate holograms could be made with this interferometer. These zone plates were limited to interference between a plane wave and a spherical wave. In this section we will analyze this interferometric system in a simple, very general fashion using the Newtonian lens equation for cascaded lens systems[8]. Then we will further generalize this system to produce zone plates with arbitrary conjugate focal planes.

The interferometer of Fig. 1 consists of two beams, the object and reference beams, labeled **O** and **R** respectively. The object beam passes through four lenses. L_1 - L_4 While the reference beam passes through all four of these lenses, it is affected only by the two achromatic glass lenses L_2 and L_4. This is a result of selecting only the zero order from L_1 and L_3, which are zone plate lenses. Thus we have two lens systems to be analyzed under the requirements for achromaticity. The easiest to analyze is the reference beam. The lenses L_2 and L_4 are in the afocal position so that when a plane wave enters from the left it exits as a plane wave to the right. Thus, the source, which is at infinity, is imaged to infinity. The radius of curvature of this beam we call r_2 and is in this case infinite. The object beam is more complicated. A point source at infinity is imaged, by the four lens system, to a plane located by D as seen in Fig. 3. D is given in terms of the focal lengths of the four lenses by

$$D = f_1 + f_2 - f_2^2/f_3 \qquad (3).$$

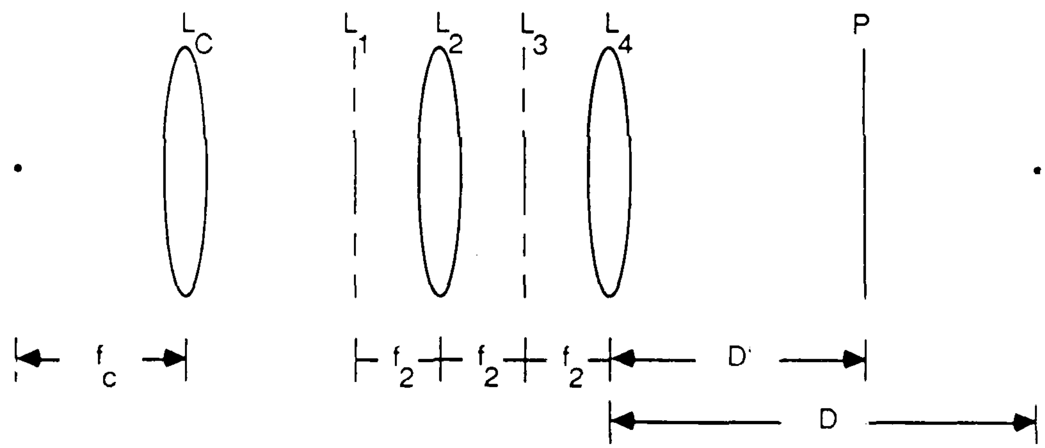

Fig. 3 The Four lens system. L_c is a collimating lens with focal length f_c. L_1 has focal length f_1. L_2 and L_4 have focal length f_2, and L_3 has focal length f_3.

D is a function of wavelength. This is a result of the two zone plate lenses L_1 and L_3 whose focal lengths, f_1 and f_3, vary with wavelength in the following manner

$$f_1 = f_{10}\lambda_0/\lambda \qquad (4)$$

$$f_3 = f_{30}\lambda_0/\lambda \qquad (5)$$

Here the subscript zero is used to represent values of the focal length at the center wavelength λ_0. Now we substitute these expressions into Eq. 3, allowing the wavelength, λ, to be expressed as

$$\lambda = \lambda_0 + \Delta\lambda \qquad (6).$$

The source image location is now given by

$$D = f_{10}[1/(1 + \Delta\lambda/\lambda_0)] + f_2 - (f_2^2/f_{30})(1 + \Delta\lambda/\lambda_0) \qquad (7).$$

Using a narrowband approximation we write

$$f_1 = f_{10}[1/(1 + \Delta\lambda/\lambda_0)] \approx f_{10}\,(1 - \Delta\lambda/\lambda_0) \qquad (8).$$

Substituting Eq. 8 into Eq. 7 we obtain the final expression for D.

$$D \approx (-2f_2^2 + f_2 f_{30})/f_{30} + (f_{10} + f_2^2/f_{30})(1 - \Delta\lambda/\lambda_0) \qquad (9)$$

We note that the second half of the Eq. 9 is of the same form as Eq. 8, i.e. the second half is inversely proportional to wavelength. This is exactly the form for the radius of curvature which is required to achromatize the fringe pattern. Thus, r_1, the radius of curvature of the object beam is

$$r_1 = (f_{10} + f_2^2/f_{30})(1 - \Delta\lambda/\lambda_0) \qquad (10),$$

where

$$(1 - \Delta\lambda/\lambda_0) \approx 1/(1 + \Delta\lambda/\lambda_0) = \lambda_0/\lambda \qquad (11).$$

With this approximate form the radius of curvature of the object beam satisfies the requirements for achromaticity. If a recording plate is placed in the plane D', as seen in Fig. 1, where D' is just D minus r_1 given by

$$D' = (-2f_2^2 + f_2 f_{30})/f_{30} \qquad (12),$$

one is able to record an off axis zone plate in polychromatic illumination. Physically we can interpret this with the help of Eq. 13 which describes the resultant fringe pattern. The wave number, k, must be constant for all wavelengths at the plane located by D'.

$$2 + 2\cos(kx^2) \qquad (13)$$

The wavelength bandwidth of the illuminating source is limited since the analysis is only approximate.

One can see from the above equations that Collins' achromatic Fourier transform analysis is a special case of the above analysis. If the radius of curvature, r_1 (Eq. 11), is set equal to zero one obtains the condition

$$f_{10} = - f_2^2/f_{30} \qquad (14).$$

This is precisely the condition obtained by Collins. A radius of curvature of zero describes the source image plane as being wavelength independent; since the Fourier transform occurs at the plane where the source is imaged the above statement, $r_1=0$, implies that the Fourier transform is also achromatic. This result supports the analysis and the analysis itself provides a more general form for achromatizing the system for Fraunhofer or Fresnel holography. The next step is to describe an optical system which allows the interference of waves of arbitrary curvature rather than being restricted to a plane wave and a spherical wave.

A Three Lens System

The three lens system of Fig. 4 is capable of forming zone plate holograms with beams of arbitrary curvature. It is essentially identical to the four lens system without the fourth achromatic lens, L_4. This is a result of the fact that the final achromatic lens serves only to image from one plane to another plane in the optical system. Thus, if the light emerging from lens L_4 forms, at some plane, an achromatic interference pattern, this plane can be regarded as the image, formed by L_4, of an object plane elsewhere, in which the two object beams also combine achromatically. The magnification will be different, thus the zone plate recovered at this other plane will be differently scaled. Also, in general, the two interfering waves will have finite radius of curvature.

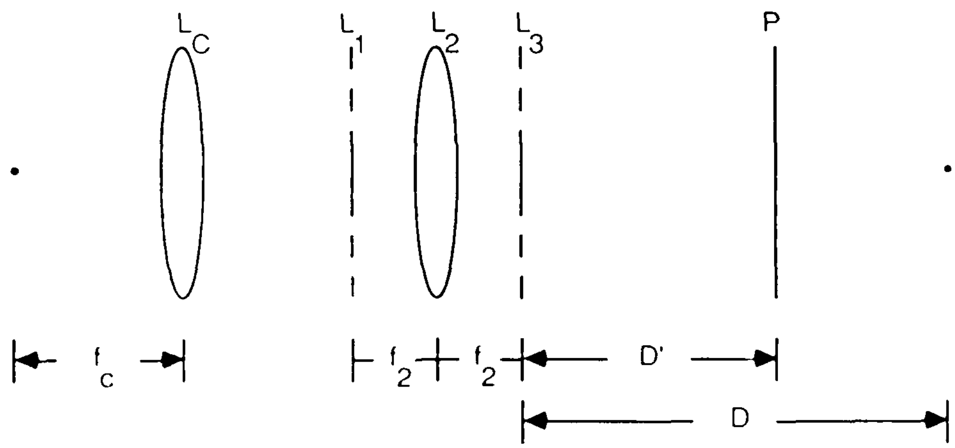

Fig 4 The three lens system. L_1 has focal length f_1, L_2 has a focal length f_2, and L_3 has focal length f_3

The analysis of the three lens system proceeds in the same manner except that now both beams have curvature. Expressions for the radius of curvature of the interfering wavefronts must be obtained for both beams. Proceeding as before, finding the source image with the point source as the object located at infinity, one finds the radii of curvature, with reference to Fig. 4, to be

$$r_1 = f_3 f_2^2/(f_2^2 - f_1 f_3) - d \tag{15}$$

$$r_2 = d \tag{16}$$

The plane located by d is the interference plane to be determined by the requirements for achromaticity. Applying these reqirements one first needs the sum of the inverses of the radii of curvature which upon substituting wavelength dependence becomes

$$1/r_1 + 1/r_2 = (\lambda/d\lambda_0)[1 + f_{10}d/f_2^2 - d/f_{30} + (\Delta\lambda/\lambda_0)(1 - 2d/f_{30} - d\Delta\lambda/f_{30}\lambda_0)] \tag{17}$$

We ignore the wavelength squared term, assuming a narrowband approximation, yielding the result

$$1/r_1 + 1/r_2 = (\lambda/d\lambda_0)[1 + f_{10}d/f_2^2 - d/f_{30} + (\Delta\lambda/\lambda_0)(1 - 2d/f_{30})] \tag{18}$$

The sum is proportional to wavelength only when the plane located by d is at

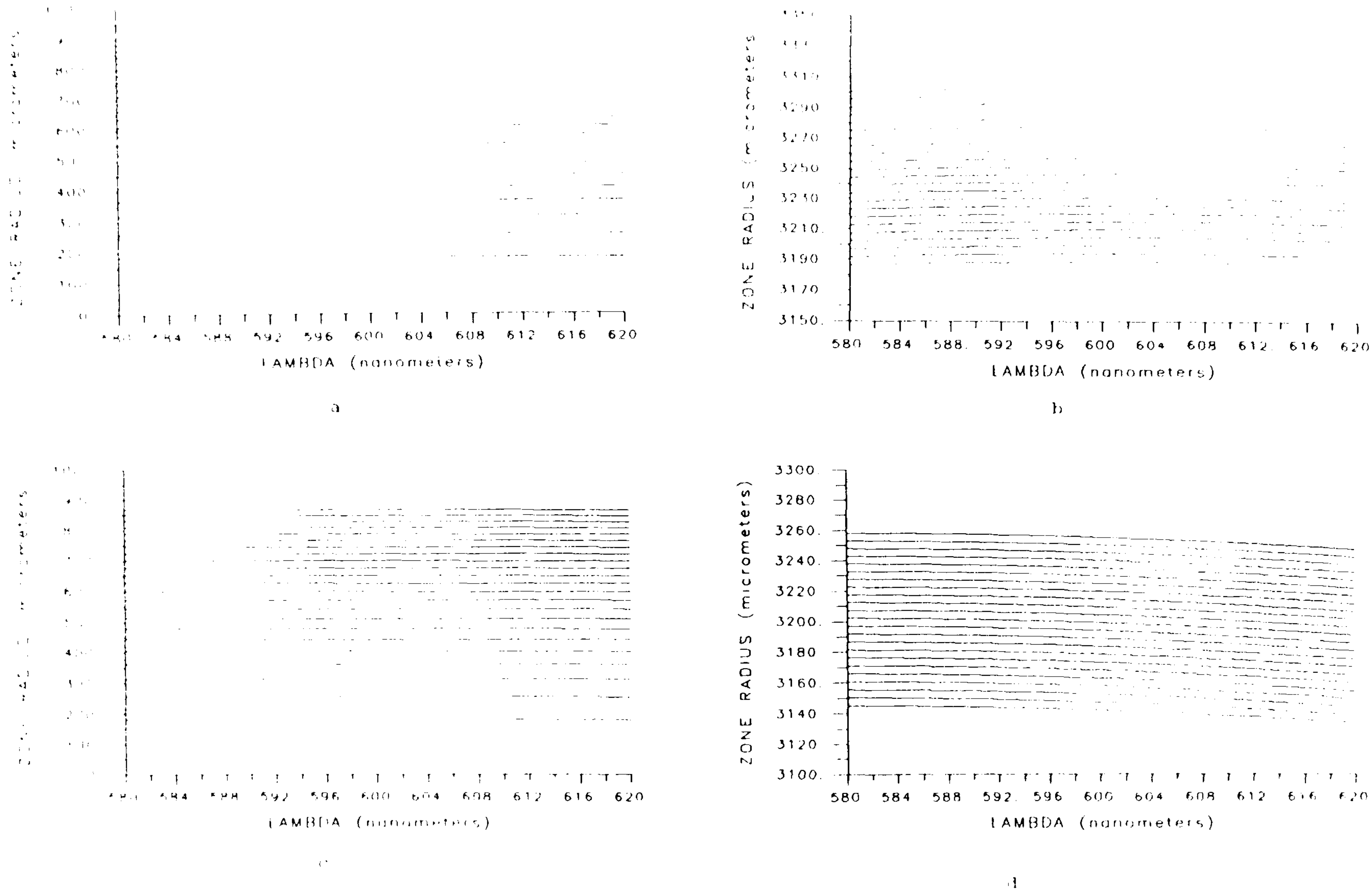

Fig. 5 Graphs (a)-(d) demonstrate the achromatization of the fringe pattern as a function of the recording plane location. The graphs are solutions of Eq. (19) for R_m as a function of wavelength. Graphs (a) and (b) are for R_m when the recording plane is that described by the achromatization. Graphs (c) and (d) are identical except that they are three millimeters out of the recording plane. The first twenty-three zones are described by (a) and (c), while (b) and (d) are for m=301-323. *It is evident that the location of the recording plane is crucial* since the zones in graph (d) have overlapped as a function of wavelength whereas those of graph (b) have not.

$d = f_{30}/2$. This is the plane where the HOE will be formed. Again the fringe pattern will only be approximately achromatic and the recording will be limited to some bandwidth. Discussions of these limitations will be found in a later section.

It is necessary to make a few restrictions on the optical system in order to insure that we interfere a converging with a diverging wave. These restrictions are taken care of by ensuring that both r_1 and r_2 are greater than zero. This is done by proper choice of the optical system parameters f_1, f_2, and f_3. With this optical system one is able to construct holographic optical elements with a wide range of conjugate focal planes and a high signal to noise ratio is obtained by use of a broad spectral bandwidth.

Limitations of Polychromatic Light

In designing HOEs in broad spectrum light one must keep in mind the consequences of increasing the spectral bandwidth. The space bandwidth product (SB) of the HOE is decreased significantly. However, the resulting SB product is adequate for most purposes. Using the equation

$$(R_m^2+r_1^2)^{1/2} + (R_m^2+r_2^2)^{1/2} - r_1 - r_2 = m\lambda \qquad (19),$$

where r_1 and r_2 are functions of wavelength as in Eq. (15) and (16) and R_m is the radius of the m^{th} zone, a SB product can be determined. Using numerical techniques, we can solve the above equation for R_m. For this example we used f_{10}=-15 cm., f_2=30 cm., and f_{30}=15 cm. The graphs in Fig. 5 show how R_m varies with wavelength for each integer m. If we allow for a 1% error in the periodicity of R_m, that is if

$$R_{m,max}(\lambda) - R_{m,min}(\lambda) < [R_m(\lambda_0) - R_{m-1}(\lambda_0)](.01) \qquad (20)$$

we can write the SB product as

$$SB = R_m/(R_m - R_{m-1}) \qquad (21).$$

With a bandwidth $\Delta\lambda$ =400 Å and λ_0=6000 Å we get an SB product of 643. A typical polychromatic interference pattern of this bandwidth has a SB product of approximately 50 (given by SB $\approx 4\lambda o/\Delta\lambda$). The compensated optical system is a factor of ten better with an F# of 4.3. There is much to gain in terms of signal to noise ratio when using polychromatic illumination. The penalty, in terms of SB product, is not too severe.

REFERENCES

1. G. J. Swanson, "Interferometric Recording of High Quality Zone Plates in Spatially Incoherent Light," Opt. Lett. **8**, 45 (1983).
2. E. N. Leith and S. Leon, "Construction and Evaluation of HOEs Made in Light of Reduced Coherence," Appl. Opt. **23**, 942 (1984).
3. S. Leon and E. N. Leith, "Optical Processing and Holography with Polychromatic Point Source Illumination," Appl. Opt. **24**, 3638 (1985).
4. R. H. Katyl, "Compensating Optical Systems. Part 1: Broadband Holographic Recocstruction; Part 2: Generation of Holograms with Broadband Light; Part 3: Achromatic Fourier Transformation," Appl. Opt **11**, p. 1241, p. 1248, p. 1255, (1972).
5. G. D. Collins, "Achromatic Fourier Transform Holography," Appl. Opt. **20**, 3109 (1981).
6. R. W. Meier, "Magnification and Third-Order Aberrations in Holography," J. Opt. Soc. Am. **55**, 987 (1965).
7. E. N. Leith and G. J. Swanson, "Achromatic Interferometers for White Light Optical Processing and Holography," Appl. Opt. **19**, 638 (1980).

4

Source-Image Distortion Description of Broad Source Fringe Formation

Introduction

Interferometry with non-coherent light is of great interest to researchers in the field of optics[1-29]. The reason for this are twofold; the first is a vastly increased signal to noise ratio over use of coherent light and the second is to be able to operate interferometers in real world situations (i.e. under ambient illumination). There are three classes of interferometers which use non-coherent or partially coherent light. First, there are interferometers which operate in polychromatic point source illumination[1-6]. Second, are interferometers which operate in illumination of reduced spatial coherence[7-17]. And third, there are interferometers which operate under illumination that lacks both spatial and temporal coherence[18-29]. This paper discusses the second class of interferometer, that is an interferometer that operates under spatially incoherent (or spatially extended source) illumination.

The interferometers of concern here split the amplitude of the incident light into two beams that arrive at the fringe formation plane (output plane) from different directions. As seen from the output plane, there are two apparent sources, each an image of the actual source. For an extended source, all points on the actual source are incoherent with each other, a property that carries over to the two source images. However, each point source on the one image has a point on the other image with which it is coherent; these two coherent points are each an image of the same actual source point. These corresponding point pairs form interference fringes. If extended source fringes are to be formed, the coherent pairs should all form identical fringe patterns.

If two such point-pair-coherent sources impinge from different directions, the various coherent point pairs produce fringes that generally are of somewhat different spatial frequency and may have phase differences that produce fringe patterns that are displaced or out of phase with each other. For example, the coherent pairs (a,a' and b,b') of Fig. 1 may produce fringes of the same spatial frequency, but the fringes due to one pair might be shifted relative to those from the other. Also, even if the angular separation of the point pairs is the same for each set, the fringes will generally not be of equal spacing. For example, suppose the pair aa' produces beams impinging symmetrically on the fringe plane P, whereas the point pair bb'

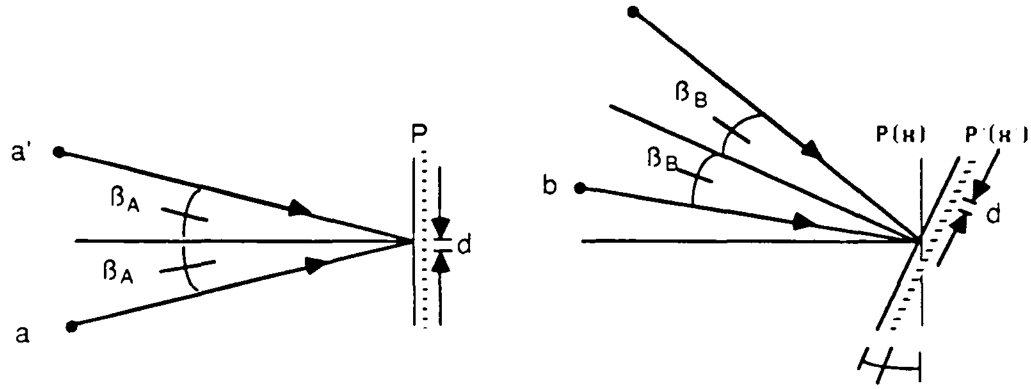

Fig. 1

does not. The fringe spacing will be less in latter the case. This becomes obvious if we consider a plane P' perpendicular to the bisector of the beams from b and b'. In this plane the fringe spacing will be d, but the fringe pattern in the plane P will be a projection, $d \cdot \cos(\Delta\beta)$, where $\Delta\beta$ is the angle between P and P'. It is evident, then, that to have perfect fringe contrast with an extended source, the two apparent-source images must be distorted in some appropriate way, so that point pairs from off-axis source points have angular separations that increase as a function of the off-axis position of the actual source point.

Our aim is to characterize the required source-image distortion, and to show that certain interferometers achieve this distortion exactly, whereas some achieve it only approximately, in varying degrees. Conventional interferometers, such as the Mach-Zehnder or Michelson, formed from mirrors and beam splitters have no distortion at all in their source images, which results in very poor extended source source fringe formation capability. We consider symmetrical and asymmetrical grating interferometers, as well as a hybrid formed from gratings or mirrors with prisms.

We find that the source distortion factor can be an indicator of the inherent extended source fringe forming capability of the interferometer.

Interferometers that fail to produce the ideal source distortion factor may be operated under conditions of reduced spatial incoherence, particularly if a source structure factor can be found that optimizes their fringe forming capability. An example of this is the Mach-Zehnder interferometer, whose extended source capability was discussed by Bennett[5] and Swanson[26]; the latter found that the Mach-Zehnder has an optimum fringe forming capability when illuminated by a continuous ring of point sources that lie at a constant radius from the optic axis. The concern here is not with the optimum source structure for a given interferometer, rather this paper poses the question: What two source image structures, that have point by point coherence between each source, create a perfect parallel fringe pattern? It is clear from Bennett's paper and Swanson's thesis that mirrors and beam splitters, that produce two exact replicas of the original source at specific locations with reference to some interference plane P, do not produce a spatially invariant fringe pattern. The ideal optical system that is needed will split the light into two beams and then recombine them at some plane to form a set of parallel fringes for a spatially extended source of any size.

Ideal Extended Source Structure

The analysis that follows assumes that the illuminating source is located at infinity, so that each source point can be considered to be mapped into a plane wave of infinite extent. It is a well known fact in coherence thoery that if an infinite field is completely incoherent in one plane, it is completely incoherent in every other plane. Thus, to the extent that the source can be approximated as infinite, there is no loss of generality in assuming a source at infinity, even if the actual source is not.

Consider two sources in space as shown in Fig. 1. The sources are assumed to be located at the back focal plane of a collimating lens with the center of each source located symmetrically about the central axis, as seen in Fig. 1. This arrangement is to be analyzed with two coordinate systems. Two sets of plane waves, each set emanating from a different point on the extended source, have been split by some optical system and are brought together at some plane P. These plane waves create fringe patterns described by the equations

$$I_A = 2 + 2\cos[4\pi x \sin(\beta_A)/\lambda + P_A] \qquad (1)$$

$$I_B = 2 + 2\cos[4\pi x' \sin(\beta_B)/\lambda + P_B] \qquad (2)$$

β_A and β_B are assumed to be different since it is apparent that if they are equal, as in the Mach-Zehnder interferometer, the fringe pattern is space variant. The consequnce of this is a distortion in the angular location of each source point. This distortion is needed in order to obtain a spatially invariant fringe pattern. The source point associated with Eq. 1 is assumed to be the zero spatial frequency component of the source, i.e. the source point on axis. This simplifies the analysis and is still completely general since the source point associated with Eq. 2 could be any source point.

The two fringe patterns must have the same spatial frequency in the x coordinate system. The relationship between these two fringe patterns is found by rotating the x' coordinate system to the x. The result of this gives x' in terms of x as

$$x' = x\cos(\Delta\beta) \qquad (3),$$

where $\Delta\beta$ is the angle between the two coordinate systems. From this the relationship between the spatial frequencies becomes

$$\sin(\beta_A)\cos(\Delta\beta) = \sin(\beta_B) \qquad (4).$$

If this relationship is satisfied the spatial frequency of each fringe pattern associated with a particular source point is equal when rotated to the x coordinate plane.

The above condition (Eq. 4) is not enough to ensure that the extended source fringe pattern is perfect, i.e., all source elements must form identical fringe patterns. Not only must all source elements form fringe patterns of the same spatial frequency, but the fringes must also be in registry. Thus, the relative phase between each fringe pattern must be zero or some integral number times 2π. Upon examining Eqs. 1 & 2 this relationship can be expressed as

$$P_A - P_B = 2m\pi \qquad m = 0, \pm1, \pm2, \pm3 \ \ldots \qquad (5).$$

Where P_A and P_B are phase constants associated with the pathlength from the source to the output plane P. This condition says that the difference in optical pathlengths for any source point pair must be zero or an integral number of wavelengths.

If an optical system is able to split and recombine light in accordance with Eqs. 4 & 5 it will produce a fringe pattern when illuminated by a spatially incoherent source of infinite extent. The distortion needed to produce this fringe pattern is evident from Eq. 3. The angular separation between each plane wave pair, $2\beta_A$ and $2\beta_B$, must be different in order to produce coincident fringe patterns in the x coordinate system. Typical reflective interferometers, such as the Mach-Zehnder, will not produce any distortion in the source and will be limited to smaller sources. Refractive optical elements such as a Fresnel biprism can be used to recombine light in a manner which distorts the source. Similarly, grating interferometers can do the same. Thus, these interferometers have the potential for forming extended source fringes, whereas the Mach-Zehnder type, which uses mirrors to achieve their result, have considerable limitations in their extended source fringe formation capability.

The Grating Interferometer

An optical system that will distort the projected source angle can be realized with the grating interferometer of Fig. 2. This fringe forming system bends light depending on the sine of the angle of incidence and it is this property that causes distortion when the sources are projected back as in Fig. 1. The basic grating equation is

$$\sin(\beta_i) + \sin(\beta_t) = \lambda f \qquad (6).$$

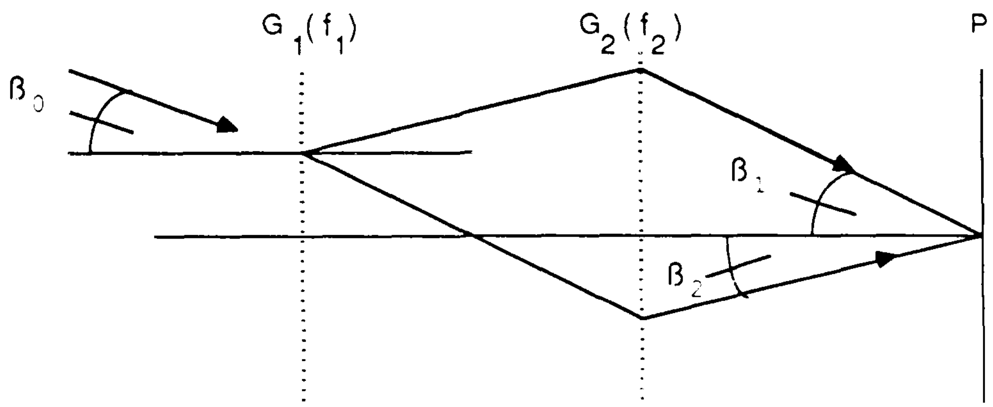

Fig 2. Gratings G1 and G2 have spatial frequency f_1 and f_2 respectively.

The angles in Eq. 6 are seen in Fig. 3, f is the spatial frequency of the grating and

λ, the wavelength of the light being used.

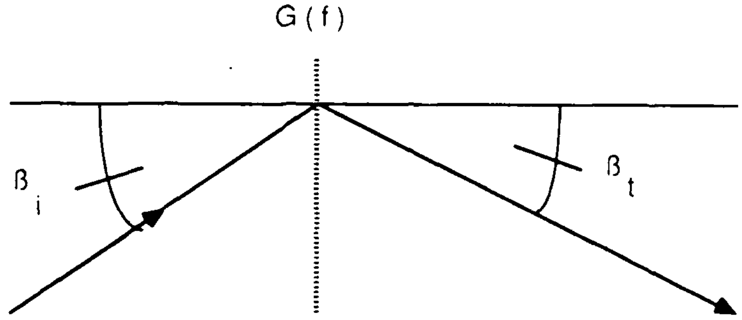

Fig 3

The angles that describe the projected source are derived using this basic equation. The resultng angular relationships, with respect to Fig. 2, are

$$\beta_1 = \sin^{-1}[\lambda(f_2\text{-}f_1) + \sin(\beta_0)] \qquad (7)$$

$$\beta_2 = \sin^{-1}[\lambda(f_2\text{-}f_1) - \sin(\beta_0)] \qquad (8).$$

These angles describe plane wave pairs due to a single source point. This source point is described by β_0, its actual angular location, and varies from zero to $\pm$ninety degrees.

Adapting these last equations two equations to Eq. 4 is an exercise in geometry. The results, given below, are easily inserted into Eq. 4 to become Eq. 12.

$$\beta_A = \sin^{-1}[\lambda(f_2\text{-}f_1)] \qquad (9)$$

$$\beta_B = (\beta_1 + \beta_2)/2 \qquad (10)$$

$$\Delta\beta = (\beta_1 - \beta_2)/2 \qquad (11)$$

$$\sin[(\beta_1 + \beta_2)/2] \bullet \cos[(\beta_1 - \beta_2)/2 = \lambda(f_2\text{-}f_1) \qquad (12)$$

Using a trigonometric identity Eq. 12 reduces to

$$[\sin(\beta_1) + \sin(\beta_2)]/2 = \lambda(f_2\text{-}f_1) \qquad (13).$$

Substituting β_1 and β_2 into Eq. 13 results in an identity. Thus, the spatial frequency of the fringe pattern produced by each point pair is exactly equal for the grating interferometer.

As previously mentioned, having the same spatial frequency fringe pattern for each point pair is not sufficient for obtaining extended source fringes. The optical pathlengths of each arm of the interferometer must have the same pathlength measured to the optical axis at the output plane P in order that fringe patterns due to each source element are in registry. The distances traveled in each arm of the interferometer for any source point is calculated by using the grating equation (Eq. 6). The distance traveled (with reference to Fig. 2) by the upper arm is given by

$$D_1 = d_1/\{1 - [\lambda f_1 - \sin(\beta_0)]^2\}^{1/2} + d_2/\{1 - [\lambda(f_2 - f_1) + \sin(\beta_0)]^2\}^{1/2} \qquad (13)$$

and the lower arm by

$$D_2 = d_1/\{1 - [\lambda f_1 + \sin(\beta_0)]^2\}^{1/2} + d_2/\{1 - [\lambda(f_2 - f_1) - \sin(\beta_0)]^2\}^{1/2} \qquad (14)$$

D_1 and D_2 are exactly equal when d_1 is equal to d_2 and f_2 is equal to two f_1. In this symmetric configuration the grating interferometer is capable of producing perfect fringes in extended source illumination.

The source distortion is achieved by the nature of the gratings and is shown graphically in Fig. 4.

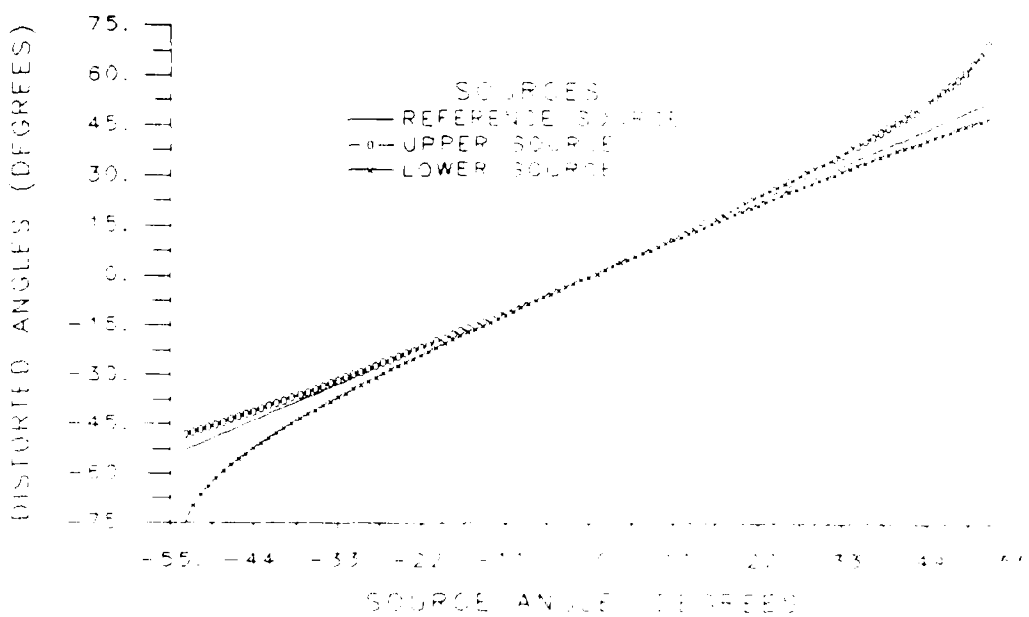

Fig. 4. The graph shows the distortion provided by the grating interferometer to obtain perfect extended source fringes. Upper source refers to the upper arm of the interferometer and lower source refers to the lower arm.

Possibilities for source distortion with other optical elements, such as the Fresnel biprism, suggest that there are other ways of obtaining perfect fringe patterns in spatially incoherent light other than by use of the grating interferometer.

REFERENCES

1. R. H. Katyl, "Compensating Optical Systems. Part 1: Broadband Holographic Recocstruction; Part 2: Generation of Holograms with Broadband Light; Part 3: Achromatic Fourier Transformation," Appl. Opt. **11**, p. 1241, p.1248, p. 1255, (1972).
2. E N. Leith and B. J. Chang, "Image Formation with an Achromatic Interferometer," Opt. Comm. **23**, 217 (1977).
3. G. D. Collins, "Achromatic Fourier Transform Holography," Appl. Opt. **20**. 3109 (1981).
4. S. Leon and E. N. Leith, "Optical Processing and Holography with Polychromatic Point Source Illumination," Appl. Opt. **24**, 3638 (1985).
5. F. D. Bennett, "Optimum Source Size for the Mach-Zehnder Interferometer," J. Appl. Phys. **22**, 184 (1951).
6. E. N. Leith, G. Collins, I. Khoo, and T. Wynn, "Correlation Image Formation with an Axicon," J. Opt. Soc. Am. **70**, 141 (1980).
7. E. Leith, H. Chen, G. Collins, K. Scholten, G. Swanson, and J. Upatnieks, "Interferometric Construction of Circular Gratings," Appl. Opt. **19**, 3626 (1980).
8. E. N. Leith and G. C. Yang, "Interferometeric Spatial Carrier Formation with an Extended Source," Appl. Opt. **20**, 3819 (1981).
9. E. N. Leith and G. J. Swanson, "Holographic Aberration Compensation with Partially Coherent Light," Opt. Lett. **7**, 596 (1982).
10. G J. Swanson, "Interferometric Recording of High Quality Zone Plates in Spatially Incoherent Light," Opt. Lett. **8**, 45 (1983).
11. H. Chen, E. N. Leith, and Y. S. Cheng, "A Method of Image Plane Multiplex Holography," Opt. Comm. **48**, 98 (1983).
12. H. Chen and Y. S. Cheng, "Low-Noise Multicolor Archival Storage with Broad Source Interferometric Imaging," Appl. Opt. **22**, 2790 (1983).
13. G. J. Swanson, "Broad-Source Fringes in Grating and Conventional Interferometers," J. Opt. Soc. Am. **1**, 1147 (1984).
14. E. N. Leith and S. Leon, "Construction and Evaluation of HOEs Made in Light of Reduced Coherence," Appl. Opt. **23**, 942 (1984).
15. E. Leith, H. Chen, Y. Cheng, G. Swanson, and I. Khoo, "Phase Conjugation with Light of Reduced Spatial Coherence," Coherence and Quantum Optics V. 1155 (1984).
16. E. N. Leith and R. Hershey, "Transfer Functions and Spatial Filtering in Grating Interferometers," Appl. Opt. **24**, 237 (1985).
17. D. K. Angell, "Incoherent Spatial Filtering with Grating Interferometers," Appl Opt. **24**, 2903 (1985).

18. B. J. Chang, "Grating Based Interferometer," Ph.D. Thesis, U. Michigan, Ann Arbor (University Microfilms, Ann Arbor, order no. 74-25-170, 1974).
19. B. J. Chang, J. S. Chang, and E. N. Leith, "Imaging Through Scattering Media with an Achromatic Interferometer," Opt Lett. **4**, 118 (1979).
20 E. N. Leith and G. J. Swanson, "Achromatic Interferometers for White Light Optical Processing and Holography," Appl Opt **19**, 638 (1980).
21 E. N Leith, "Simultaneous Position and Velocity Measurement by Interferometric Imaging," Opt. Lett. **6**, 261 (1981).
22. G. J. Swanson, "Recording of One-Dimensionally Dispersed Holograms in White Light," Appl. Opt. **20**, 4267 (1981).
23. E. N. Leith and G. J. Swanson, "Recording of Phase-Amplitude Images," Appl. Opt. **20**, 3081 (1981).
24. E. N. Leith, H. Chen, and Y. S. Cheng, "Diffraction-Limited Imaging Through a Phase-Distorting Medium," Opt. Lett. **6**, 4 (1981)
25 G J. Swanson and E. N. Leith, Lau Effect and Grating Imaging," J. Opt. Soc. Am. **72**, 552 (1982).
26. G. J. Swanson, "Partially Coherent Imaging and Interferometry Based on Diffraction Gratings," Ph.D. Thesis, U. Michigan, Ann Arbor (University Microfilms, Ann Arbor, 1983)
27. Y. S. Cheng and E. N. Leith, "Successive Fourier Transformation with an Achromatic Interferometer," Appl. Opt. **23**, 4029 (1984).
28. Y. S. Cheng, "Fringe Formation in Incoherent Light with a Two-Grating Interferometer," Appl. Opt. **23**, 3057 (1984).
29 G J. Swanson and E. N. Leith, "Analysis of the Lau Effect and Generalized Grating Imaging," J Opt. Soc. Am A **2**, 789 (1985).

5

Generalization of Some Incoherent Spatial Filtering Techniques

Generalization of some incoherent spatial filtering techniques

Emmett N. Leith and Daniel K. Angell

A two-channel incoherent spatial filtering system is generalized by considering two object transparencies, one in each of the two channels. Various special cases result, including two that have previously been described and others not previously given. The system can be either linear in irradiance (the basic incoherent case) or linear in field (the basic coherent case) even though the illumination is incoherent in either case. In particular, we show spatial filtering with the object in one channel and the spatial filter in the other channel.

I. Introduction

Spatial filtering with spatially incoherent light has attracted considerable interest in recent years. Görlitz and Lanze, Lohmann, Rhodes and Stoner[1-6] have considered two-channel incoherent spatial filtering systems, in which the light from the object is split into two parts and separately filtered in each before recombining at the output. If H_1 and H_2 are pupil function masks placed in each of the two channels, the system transfer function is the autocorrelation function of ($H_1 + H_2$). The terms $H_1 \circledast H_1$ and $H_2 \circledast H_2$ are the components that result from conventional one-channel incoherent spatial filtering, while $H_1 * H_2$ and $H_2 \circledast H_1$, the cross-correlation of the two pupil functions, result from the presence of two simultaneous channels. Since H_1 and H_2 can be any complex function, the resulting cross-correlation will generate any arbitrary system transfer function. It appears that this procedure leads to incoherent spatial filtering systems that have the full versatility associated with the coherent counterpart.

Thus, if an object has amplitude transmittance s and irradiance transmittance $|s|^2$, the cross-product term yields an output $|s|^2 * h$, where h is the point spread function corresponding to the transfer function $H_1 \circledast H_2$. Angell[7] found significant advantages when the interferometer is formed from diffraction gratings. Collins[8] among others has noted that by placing the object in one of the beams instead of before the interferometer, the optical system becomes linear in amplitude and preserves phase, even though the light is spatially incoherent. He demonstrates the construction of Fourier transform holograms made in spatially incoherent light.

We present here an analysis that generalizes the above results.

II. Basic System

We show (Fig. 1) an interferometer formed from diffraction gratings G_1 and G_2. The upper beam is produced by the +1 order of grating G_1 and is redirected as the −1 order of the grating G_2. Similarly, the lower beam is produced as the −1 order of G_1 and is redirected as the +1 order of G_2. The beams are brought together again. Although many variants of grating interferometers are possible, we chose for our analysis the highly symmetric arrangement where gratings G_1 and G_2 have spatial frequencies of f_1 and $2f_1$, respectively. We show optical spatial filtering systems in each beam. Without these systems, the beams would simply recombine and form, under spatially incoherent illumination (either monochromatic or polychromatic), high-contrast fringes of spatial frequency $2f_1$. When the optical systems are in place, fringes become modulated with information related to the masks s_1, s_2, H_1, and H_2. The optical system in each beam is a spatial filtering system. The upper beam contains the object (or signal) transparency s_1; a second mask H_1 placed at the focal plane of the first lens is a conventional spatial filter. A similar system is placed in the lower beam with transparencies s_2 and H_2. The two beams are combined at the plane where the spatially filtered images of s_1 and s_2 form. Alternatively, the two spatial filtering systems could be one system with the two beams passing through different portions of the same lenses. For the following analy-

The authors are with University of Michigan, Ann Arbor, Michigan 48109.

Received 24 September 1985.
0003-6935/86/040499-04$02.00/0.

sis, we chose the former system, although the latter yields similar results.

III. Theory

For simplicity, the analysis is carried out in two dimensions, x and z. The other lateral dimension y is dropped; however, the analysis we develop is readily extended to the y dimension also.

Let the source be extended sufficiently so that it can be regarded as completely spatially incoherent, i.e., an infinite source. One element of the source presents a plane wave $\exp(j2\pi f_0 x)$ to the grating G_1, where $f_0 = \sin(\theta_0/\lambda)$, with θ_0 the angle of irradiance and λ the wavelength. The upper beam can be written as $\exp[j2\pi(f_0 + f_1)x]$ after exiting from grating G_1. Constant coefficients, irrelevant to the analysis, are dropped. The light impinging on G_2 has incurred a phase delay $\exp[-j\pi\lambda d(f_0 + f_1)^2]$; this is the transfer function of free space.[8] (We have thus described the light propagation in the frequency domain.) A bulk phase delay $\exp(j2\pi f_0 d)$ has been dropped. The field exiting G_2 is then $\exp j[2\pi(f_0 - f_1)x - \pi\lambda d(f_0 + f_1)^2]$.

The delay term $\pi\lambda d(f_0 + f_1)^2$ is the same for the upper and lower branches of the interferometer and may, therefore, be ignored.

Next we consider the field incident on mask s_1. The mask and the following optical system are oriented perpendicular to the ray from the center of the source; thus the term $\exp(-2\pi j f_1 x)$ is removed. The field emerging from the filter transparency is

$$H_1(f_x)\int s_1(x)\exp[j2\pi(f_0 + f_x)x]dx, \tag{1}$$

where f_x is a spatial frequency variable, $f_x = x'/\lambda F$, where x' is the physical coordinate of this plane, and F is the lens focal length. At the output, the field is

$$u_1 = \int H_1(f_x)\left[\int s_1(x)\exp[j2\pi(f_0 + f_x)x]dx\right] \times \exp(-j2\pi f_x x')df_x. \tag{2}$$

A similar analysis for the lower beam yields

$$u_2 = \int H_2(f_x)\left[\int s_2(x)\exp[j2\pi(f_0 + f_x)]dx\right] \times \exp(-j2\pi f_x x')df_x. \tag{3}$$

Since the two beams combine at nonzero angles we have the partial field due to the source element at θ_0 being

$$u = u_1\exp(-j2\pi f_1 x) + u_2\exp(j2\pi f_1 x) \tag{4}$$

with irradiance $|u|^2$. The total irradiance is found by integrating over the source:

$$I = \int|u|^2 df_0 = \int|u_1|^2 df_0 + \int|u_2|^2 df_0 + \exp(-j4\pi f_1 x) \times \int u_1 u_2^* df_0 + \exp(j4\pi f_1 x)\int u_1^* u_2 df_0. \tag{5}$$

The first term is just what would result if only the upper beam were present, the second that which results from the lower beam alone. These terms are of no interest here. The third and fourth terms are of interest. They combine to give a modulated fringe pattern of spatial frequency of $2f_1$. Since they are complex conjugates, we need examine only one of the two. The third term can be written

$$\int u_1 u_2^* df_0 = \int\left(\int H_1(f_x)\left[\int s_1(x)\exp[j2\pi(f_0 + f_x)x]dx\right]\exp(-j2\pi f_x x')df_x\right) \times \left(\int H_2^*(f_x)\left[\int s_2^*(x)\exp[-j2\pi(f_0 + f_x)x]dx\right]\exp(j2\pi f_x x')df_x\right)df_0 \tag{6}$$

Fourier transforming the integrals in parentheses yields

$$\int u_1 u_2^* df_0 = \int\left[\int H_1(f_x)S_1(f_x + f_0)\exp(-j2\pi f_x x')df_x\right] \times \left[\int H_2^*(f_x)S_2^*(f_x - f_0)\exp(j2\pi f_x x')df_x\right]df_0 \tag{7}$$

which can be rewritten as

$$\int u_1 u_2^* df_0 = \int\int\int h_1(\alpha - x')h_2^*(\beta - x')s_1(\alpha) \times s_2^*(\beta)\exp[j2\pi f_0(\alpha - \beta)]d\alpha d\beta df_0 \tag{8}$$

Integrating on f_0 produces a δ-function $\delta(\alpha - \beta)$ yielding

$$\int u_1 u_2^* df_0 = \int h_1(\alpha - x')h_2^*(\alpha - x')s_1(\alpha)s_2^*(\alpha)d\alpha \tag{9}$$

This result has several interesting special cases:

Case 1. $s_1 = s_2 = s$. This leads to the result

$$I = \int u_1 u_2^* df_0 = \int h_1(\alpha - x')h_2^*(\beta - x')|s|^2 d\alpha. \tag{10}$$

or, Fourier transforming, we obtain

$$\mathcal{F} I = S(H_1 \star H_2), \tag{11}$$

where S is the Fourier transform of $|s|^2$.

This case can be construed as the one already treated by others, where the object $|s|^2$ is placed before the interferometer, and thus is presented to both interferometer branches. The result is an incoherent spatial filtering process, where the object irradiance $|s|^2$ is modified by a transfer function that is the autocorrelation function of the pupil masks H_1 and H_2.

Case 2. $s_2 = 1$, $H_2 = \delta$-function. We obtain

$$I = s_1 \ast h_1. \tag{12}$$

In this case, the system is linear in amplitude, just as in the case of coherent illumination. However, the illumination here is spatially incoherent. In short, the incoherent system is behaving like a coherent system analogous to the system described by Collins. We obtain an arbitrary transfer function without the need

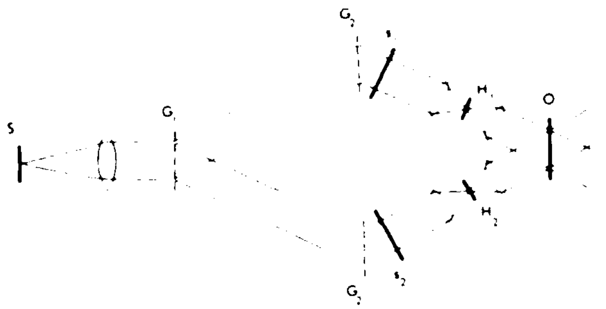

Fig. 1. Interferometer for generalized spatial filtering: S, source; G_1, G_2, gratings; s_1, s_2, objects; H_1, H_2, spatial filters; O, output plane.

for two-pupil masks. However, the system acts on the amplitude rather than the irradiance transmittance: this difference could either be advantageous or disadvantageous depending on circumstances. In particular, the process would not be effective for diffuse objects, just as a coherent spatial filter is ineffective for diffuse objects.

Case 3. $s_2 = 1$, $H_1 = \delta$-function. We obtain

$$I = s_1 * h_2 \tag{13}$$

This is an interesting and puzzling result. Coherent spatial filtering has been carried out with spatially incoherent light, as in Case 2. However, we have two optical spatial filtering systems in parallel with the object in one system and the spatial filter in the other; here the light transmitted by the object does not pass through the spatial filter, although the effect is as if it did.

If we take $H_2 = 1$, we have a simple imaging process. However, the optical system that images the object to the output has a vanishingly small aperture, hence, is supposedly incapable of image formation with any resolution. Yet the resolution can indeed be very good, since the effective aperture for the system is not the aperture of the object-bearing system but is instead the aperture of the other branch of the interferometer.

This seemingly impossible result can be explained in a simple way. We think of the source as made up of many points. The point element on-axis forms an object Fourier transform centered on the pinhole spatial filter, so that only the zero spatial frequency component of the object is passed. Another source element forms a displaced Fourier transform so that a nonzero spatial frequency component f_1, with components f_{1x}, f_{1y}, is passed. In this way, each source element passes one spatial frequency component of the object. A photographic record is then made on the output. The zero order of this record, considered as an image plane hologram, will form an image with extremely poor (or no) resolution; however, in the first diffracted order the resolution will be to be far in excess of what is possible given the pinhole aperture. How good the resolution is depends on the size of the source. The more extended (i.e., the more spatially incoherent) the source, the better will be the resolution.

Case 4. s_1, s_2, H_1, H_2 arbitrary. This case, which is described by Eq. (9), would seem to add little generality to what is offered by Case 2. We can generate any possible transfer function by a single transparency H_1. So what can be the advantage of the second H_2? We speculate that we obtain better contrast fringes and hence a stronger cross-term signal by having two transparencies. For example, for a binary filter $H_1 = 0$ or 1, we might obtain better contrast by having the second transparency and setting $H_2 = H_1$.

IV. Experimental Results

Two experiments were performed to demonstrate the theory presented here. The optical system was

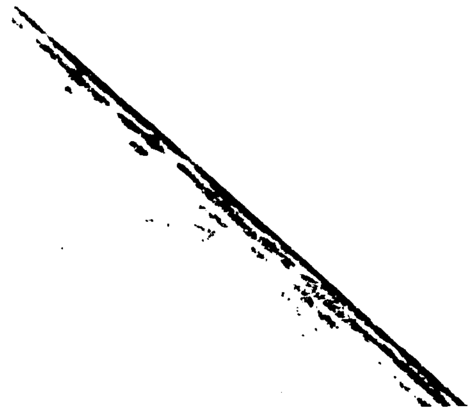

Fig. 2. Edge sharpening with incoherent source

Fig. 3. Image of straightedge formed with pinhole spatial filter in conventional one-channel imaging system

essentially that shown in Fig. 1, except that a single lens was used in each beam instead of a pair. G_1 was of 100-cycle/mm spatial frequency; G_2 was in fact two separate gratings, each of 200-cycle/mm spatial frequency. The source, formed by shining a diverging laser beam onto a rotating ground glass, was adjustable in size and for the most favorable results subtended an angle of 4.3° at the collimator. The image was formed at the output plane with 3× magnification.

The first experiment was performed to demonstrate Case 2. Edge sharpening was carried out by placing a small circular dot in the frequency plane of beam 1 (the object-bearing beam), and a small pinhole was placed in the other. The object was a straightedge. The output was recorded as an image-plane hologram and read out with a monochromatic broad light source sufficiently small that the diffracted orders could be separated. The experimental results (Fig. 2) show prominent edge sharpening, thus verifying the conclusions of Case 2.

The second experiment was to demonstrate Case 3. We show improved imaging with the introduction of a second beam, i.e., $H_2 = \delta(f_x, f_y)$ and $s_1 = 1$. The pinhole for the experiment was placed in the Fourier transform plane of the object beam. The second beam had no

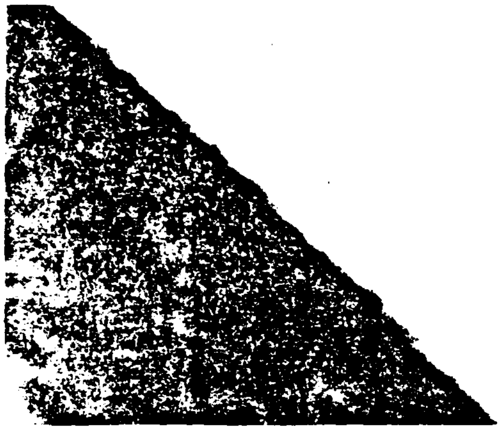

Fig. 4. Image of straightedge formed with pinhole spatial filter in object beam and no restrictive aperture in other beam.

spatial filter; hence the aperture was effectively the image of the source, which was many times larger than the pinhole. Figure 3 shows the image of the straightedge formed in the conventional way, with only one channel. As expected, the image is quite poor because of the small pinhole aperture. Figure 4 shows results obtained when the other branch of the interferometer was in operation, thereby producing a fringe pattern. This, on recording, was treated as an image-plane hologram and was read out with a somewhat extended nonochromatic light source. The image, forming in *the first diffracted order, is seen to be considerably* sharper than in Fig. 3, showing that the effective aperture is far larger than the pinhole, thus verifying the conclusions of Case 3.

This work was sponsored by the Air Force Office of Scientific Research grant AFOSR-85-0012 and by the National Science Foundation grant NSF-G-ECS-8212472.

References

1. D. Gorlitz and F. Lanzl, "Methods of Zero-Order Noncoherent Filtering," Opt. Commun. **20**, 68 (1977).
2. A. W. Lohmann, "Incoherent Optical Processing of Complex Data," Appl. Opt. **16**, 261 (1977).
3. W. T. Rhodes, "Bipolar Pointspread Function Synthesis by Phase Switching," Appl. Opt. **16**, 265 (1977).
4. A. W. Lohmann and W. T. Rhodes, "Two-Pupil Synthesis of Optical Transfer Functions," Appl. Opt. **17**, 1141 (1978).
5. W. Stoner, "Edge Enhancement with Incoherent Optics," Appl. Opt. **16**, 1451 (1977).
6. W. Stoner, "Incoherent Optical Processing via Spatially Offset Pupil Masks," Appl. Opt. **17**, 2454 (1978).
7. D. Angell, "Incoherent Spatial Filtering with Grating Interferometers," Appl. Opt. **24**, 2903 (1985).
8. G. D. Collins, "Temporally and Spatially Incoherent Methods for Fourier Transform Holography and Optical Information Processing," Ph.D. Dissertation, U. Michigan, Ann Arbor (1983); available from University Microfilms, Ann Arbor.
9. J. W. Goodman, *Introduction to Fourier Optics* (McGraw-Hill, New York, 1968), Chap. 3, p. 53.

6

Superresolution by Incoherent to Coherent Conversion

6. Superresolution by Incoherent to Coherent Conversion

The previous section discussed a variety of situations in spatial filtering with incoherent light. We showed that if the object is placed in only one branch of the interferometer (as in Fig. 1), the system acquired a number of interesting properties. We are always interested in the cross-product term, recorded on a spatial carrier, as in holography. With a signal s_1 and a spatial filter H_1 in one branch, and a signal s_2 and a spatial filter H_2 in the other branch (as in Fig. 1), the cross-product term, which is read out as the 1st diffracted order of the recorded output, has the form

$$s_1 s_2^* * h_1 h_2^* \qquad (1)$$

where the $*$ denotes convolution.

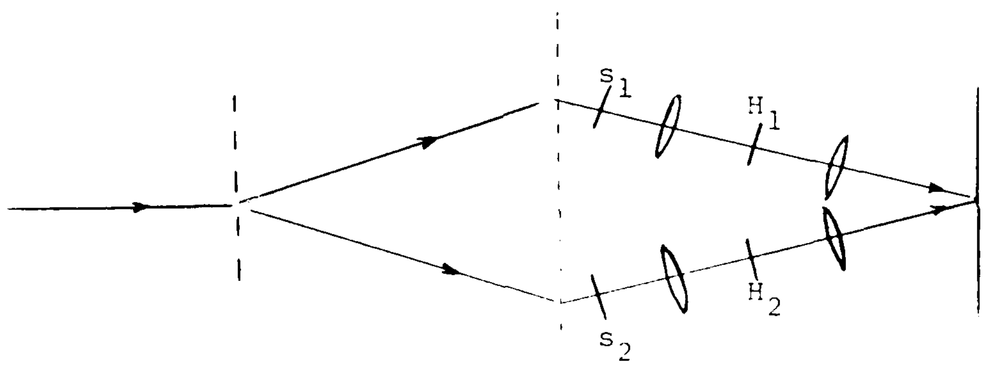

Fig. 1

If we take $s_1 = s_2 = s$, we obtain immediately the result

$$|s|^2 * (h_1 h_2^*) \qquad (2)$$

which is equivalent to the well-known case of having the object upstream from the interferometer. The system is linear in intensity, and operates with object irradiance $|s|^2$. The transfer function H is the Fourier transform of the point spread function $h_1 h_2^*$, or

$$H = H_1 \circledast H_2 \qquad (3)$$

where $\circledast$ means cross-correlation.

Other cases not as yet explored, are also possible. An interesting possibility is to have $s_2 = 1$ and $h_2 = 1$ whereupon we have an output

$$s_1 * h_1 \qquad (4)$$

This is mathematically the case of coherent spatial filtering, even though it has been carried out with spatially incoherent light. This interesting possibility is one we wish to explore. We can let H_1 be any filter that has been made for coherent illumination. It can, for example, be a holographic spatial matched filter, or a complex filter image restoration, or deblurring. We expect to obtain all of the advantages of coherent spatial filtering, along with the low noise excellent image quality associated with incoherent imaging.

Another variation of this, which is mathematically equivalent, but physically quite different, is to have $h_1 = 1$. The operation is then

$$s_1 * h_2^* \qquad (5)$$

As before, this is a coherent operation carried out with incoherent light. The object s_1 has been spatially filtered by a filter H_2 that is physically isolated; the light that emanates from the object s_1 does not pass through the mask at all, yet the mask exerts the same effect as if it were in the object light path. Here is a new concept in spatial filtering, where the signal and filter are essentially isolated.

Again, suppose $s_2 = 1$. Let the filter impulse response be binary (0 or 1), with $h_1 h_2^* = h_1 = h_2 = h$. Is there any detectable difference between having a spatial filter H in just one path or both? The mathematics suggests identical situations, but of course physically they are quite different. What advantages can arise from having H in the other channel or in both channels? Would the SNR be improved?

The most parodoxical case of all comes by letting $s_2 = 1$, $h_1 = 1$ and h_2 the desired spread function. Note that $h_1 = 1$ means $H_1 = \delta$ (a dirac delta function); this situation is depicted in figure 2.

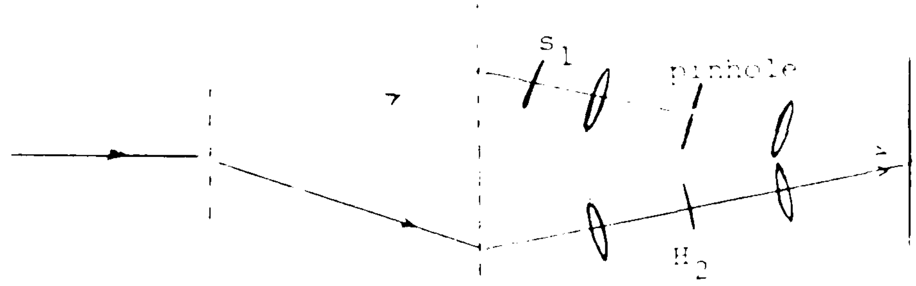

Fig. 2

If we consider the upper path as an imaging system by itself, it is a system incapable of much resolution. If the pinhole is indeed a delta function, i.e., truly a point, there is no resolution at all. If the pinhole is of a more practical size, say 10-50 microns, which is a common pinhole size, then the resolution will be extremely poor. This situation is equally true for either coherent or incoherent illumination - the resolution is not much different for these two cases. Indeed, within the framework of conventional imaging theory, the resolution simply cannot be better than the Rayleigh limit imposed by the aperture size.

Yet in this case theoreticoal considerations predict resolution equal to what one would get from an imaging system without the pinhole constriction. We thus obtain resolution far in excess of the classical limit - in short, superresolution.

One might ask, how can the resolution be that of a normal imaging system? The information needed to produce the resolution is simply not there - such information is not transmitted by the aperture. The aperture of the parallel system is adequate, but then, no object information passes through this aperture.

Techniques exist for superresolution. One common method is analytic continuation. Such techniques require nearly noise-free systems, extremely accurate measurements, and considerable computation. They can often be used to go a factor two beyond the classical limit, but seldom any further.

Are we dealing here with a similar superresolution system that would have the same limitations, or is it something quite different? We suggest the latter, and our initial experimental results support this view. Certainly, the exacting measurement and computational aspects of superresolution are absent here.

What would one expect the resolution to be in a practical system? In practice, the source will not be infinite, but of a size of the order of a centimeter. This source is imaged in beam two (Fig. 2). Now, suppose we place an iris in beam two at this source image plane. Let the iris be initially small, and we proceed to open it. As we do so the resolution is expected to improve. When the iris is the size of the source image, further enlargement lets through no additional light. Thus the effective aperture of the system is the size of the source image. Or put equivalently, the effective f-number of the imaging system depends upon the angle the source substends at the collimator. The larger the source, the larger the effective aperture, and the better the resolution.

Carrying this viewpoint further leads to the conclusion that this system is essentially different from other superresolution techniques. We show that the gain in resolution does come at a price, but at a fairly modest one.

An incoherent (or partially coherent) system can be considered as the superposition of many coherent ones; each source element gives rise to a separate channel with its own independent noise. If the optical system remains the same, the number of resolvable elements in the image is the number of effective coherent sources, and hence the number of independent channels. One would expect the incoherent system to have a SNR improvement of the $N^{1/2}$ over the coherent case, where N is the number of channels. In practice, the improvement is enormously less than this, since the noise produced by adjacent or nearby channels would not be independent, particularly for noise of components of low spatial frequency.

The above optical system in effect converts the incoherent system into a coherent one in the following way. The center element of the source forms, at the pinhole aperture of channel 1 , a Fourier transform of the object s. The pinhole allows only the 0 spatial frequency to pass. Similarly an off-axis element projects a displa or off-axis Fourier transform to the pinhole, and a nonzero spatial frequency asses. Thus, the number of spatial frequency components that pass is the number of resolvable source elements as seen from the Fourier transform plane. For an incoherent system, these contributions would combine incoherently and would loose their identity as different spatial frequency components of the object. But in the above case, they combine coherently, even though the source elements are completely incoherent. The effect is that of a source the size of pinhole, and an imaging aperture the size of the source.

This tradeoff can often be highly favorable, since experience shows that moderate reduction of redundancy due to incoherency generally leads to no observed degradation of the image. The number of redundancy channels in the output system can be of the order of 10^6 and reducing this to an order 10^3 typically does not make much difference, either in practice or in theory. In practice the difference is far less than in theory, since closely adjacent channels carry only partially uncorrelated noise, ie.e, low spatial-frequency noise components would be almost identical for adjacent channels.

This appears to be a basically new concept in superresolution: superresolution by incoherent to coherent conversion. The discovery of this concept was rather serendipitous, and we have since pondered on what its implications may be, and on what usefulness it can have. We raise several pertinent questions:

1. Can it be used to overcome aberrations? For example, the imaging system carrying the information is operated at high f-number (a consequence of the pinhole) and therefore will have low aberration. The reference imaging system operates at low f-number, but with a very narrow field. Hence, the overall imaging process may be better than the comoponent lenses would ordinarily allow.
2. Can the process be achromatized, so that it can be carried out in polychromatic light with the possibility of tradeoff of temporal incoherency for resolution?
3. How can the basic system be modified and extended so as to lead to practical applications?
4. Can we use the system in a situation where high light levels, used in one branch, can be spatially filtered with low light levels in the other branch?

7. Journal Articles Prepared or Published This Year

1. S. Leon and E. Leith, "Optical Processing and Holography with Reduced Coherence Polychromatic Point Source Illumination," Appl. Opt. 24, 3638 (1985).
2. E. Leith and D. Angell, "Generalization of Some Incoherent Spatial Filtering Techniques," Appl. Opt. 25, 499 (1985).

Some papers almost ready for submission

3. S. Leon and E. Leith, "Generalization of the Two-Zoneplate Method of Achromatized HOE Formation," (Cpt. 3 of this report). Will shortly be submitted to Applied Optics.
4. S. Leon and E. Leith, "Source-Image Distortion Description of Broad Source Fringe Formation," (Cpt. 4 of this report). Will shortly be submitted to Applied Optics.

5. E. Leith and D. Angell, "Superresolution by Incoherent to Coherent Conversion," (Cpt. 6 of this report). Will shortly be submitted, probably to J. Opt. Soc. Am.

8. Persons Associated with this Effort

E. Leith (PI)

S. Leon (Graduate Student)

D. Angell (Graduate Student)

9. New Discoveries

Of our various accomplishments, one stands out as being of special interest. This is our discovery of a new type of imaging system, in which the optical transfer function of the imaging process is controlled by the optical transmission characteristics of a parallel channel, through which light from the object does not go. A dramatic example of this is obtained by using a very small aperture in the imaging channel, and a larger aperture in the other channel. Resolution far beyond the diffraction limit is obtained. We believe this to be an astonishing result, wholly new.

END

DTIC

7-86